JOURNAL OF AIRCRAFT
Vol. 29, No. 3, May–June 1992

Numerical Simulation of Leading-Edge Vortex Breakdown Using an Euler Code

P. J. O'Neil,* R. M. Barnett,† and C. M. Louie‡
McDonnell Aircraft Company, McDonnell Douglas Corporation, St. Louis, Missouri 63114

Reliable simulation of the breakdown of leading-edge vortices emanating from sharp leading edges of delta wings is demonstrated using an Euler code. A straightforward technique is described that identifies the onset of vortex breakdown within numerical solutions, thereby allowing quantitative comparison with experimental data. Predictions of breakdown progression with angle of attack are shown to be consistent with test data up to $C_{L_{max}}$, and indicate that the vortex breakdown process is governed primarily by inviscid factors. Effects of computational grid characteristics and wing camber effects on breakdown prediction are also noted.

Introduction

As more powerful computers become available, the use of computational fluid dynamic (CFD) codes is becoming more prevalent in the early stages of the aerodynamic design process. However, the accurate modeling of viscosity-dominated flow effects (e.g., separation, vortex core structure, shock-boundary-layer interaction, etc.) is still well outside the reach of routine engineering design application. The computational resource requirements alone make three-dimensional Navier-Stokes computations prohibitive for most preliminary design tasks. On the other hand, Euler methods have demonstrated their usefulness in the design environment for a wide variety of applications where the inviscid flow assumption is appropriate. An area that has generated considerable interest and controversy is the practical reliance on Euler codes for predicting the aerodynamic consequences of vortex-dominated flowfields. Although limited by the inviscid flow assumption, Euler methods can simulate the formation of a free shear-layer from the sharp edge of an aerodynamic surface. Depending on the incidence of the edge with respect to the freestream, the free shear-layer may then roll-up to form a vortex core.[1-3] In some cases, Euler solutions have exhibited, over highly swept wings, a rapid loss of the well-defined vortex structure resembling qualitatively, vortex breakdown.[4-6] It is only recently that occurrences of such breakdown-like effects in Euler solutions have been treated with more than a passing interest.[7,8]

Complicating the interpretation of these vortex breakdown-like effects in Euler solutions is the general lack of understanding of the mechanisms that govern the vortex breakdown process. Many have shown that the essential vortex flow features leading to breakdown-onset can be successfully modeled using inviscid approximations to the fluid dynamics.[9,10] If breakdown is governed primarily by inviscid factors then an appropriate question is: Can an Euler code routinely predict such effects under the influence of arbitrary levels of numerical dissipation that are inherent to such solutions? To explore these issues, an effort was initiated to determine, through a systematic and quantitative approach, the ability of CFD codes to simulate complex vortical flow phenomena including vortex breakdown. The work reported here relates specifically to vortex breakdown prediction using Euler codes.

Presented as Paper 89-2189 at the AIAA 7th Applied Aerodynamics Conference, Seattle, WA, July 31–Aug. 2, 1989; received Aug. 31, 1989; revision received May 13, 1991; accepted for publication May 14, 1991.

*Unit Chief, Technology. Senior Member AIAA.
†Senior Engineer, Technology. Member AIAA.
‡Senior Engineer, Technology.

Background

The computational problem selected for this study was that of a delta wing planform at angles of attack sufficient to produce leading-edge vortex formation. The delta geometry yields the important vortical flowfield features yet allows straightforward computational grid generation and CFD analysis. Euler code predictions of flow separation location on rounded leading edges have been shown to be influenced by computational factors.[2] Therefore, this analysis has been restricted to sharp-edged delta wings where the location of leading-edge shear-layer separation is fixed at the physically correct position.

The primary experimental database used in this study was the MDC/NADC vortex flowfield investigation.[11] This database was developed in the McDonnell Douglas Research Laboratory (MDRL) Shear Flow Facility and consists of a very comprehensive array of three-dimensional laser Doppler velocimetry measurements (LDV), surface pressures, off-body total pressures, and laser light-sheet flow visualization data. Figure 1 shows sketches of the 60-deg and 70-deg semispan delta wings that were used to develop the data base. Both wings were flat plates having 25-deg leading- and trailing-edge bevels on the lower surface. Thus, shear-layer separation occurs at the leading edge of the flat upper surface. More complete descriptions of the wind-tunnel test program and its associated database can be found in the papers of Kegelman and Roos.[12,13]

The CFL3D Navier-Stokes code was applied in the Euler mode at Mach 0.2, to generate solutions corresponding to selected angles of attack in the experimental database.[14] The computational algorithm in CFL3D is based on a thin-layer approximation to the three-dimensional, time-dependent, compressible Navier-Stokes equations. The code is formulated as a cell-centered, finite-volume, upwind-differencing method. An input flag allows the user to execute CFL3D in the Euler mode. For a given grid, CFL3D offers no user control over the application of numerical dissipation in the solution process, and there were no explicit attempts in this analysis to affect the solutions through such means. In each case, CFL3D was run in a local time-step mode to speed the convergence to a quasisteady flowfield solution.

The SCRAMG grid generation package, described by Verhoff and O'Neil, was used to create the grids for the Euler analysis.[15] The grid generation method used here evolved from the method of Thompson et al., which solves an elliptic system of partial differential equations.[16] Forcing functions allow strong localized control of node spacing and grid orthogonality on or near grid boundaries. For the H-O topology used, each delta-wing grid was constructed by successive generation of two-dimensional grids (0 topology) at each root-chord station of interest. The two-dimensional grid code automatically sections the cross-plane domain into a number of

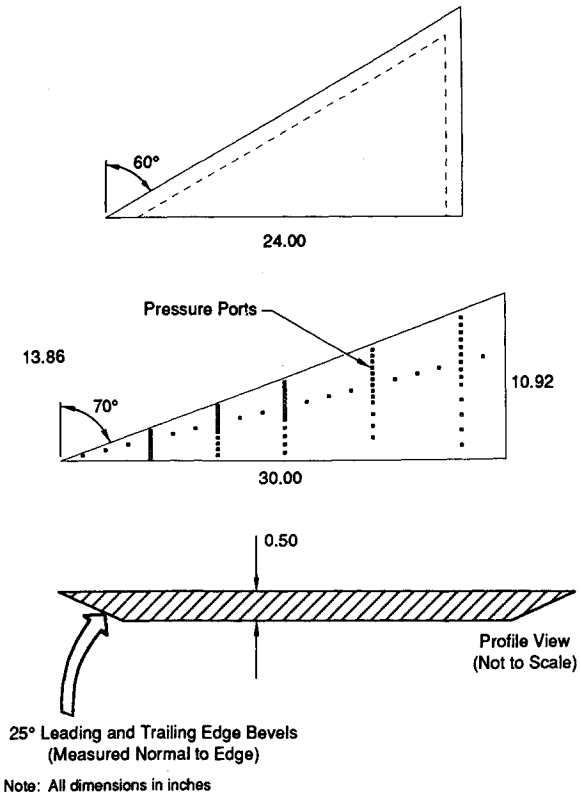

Fig. 1 Flat plate semispan delta wing models.

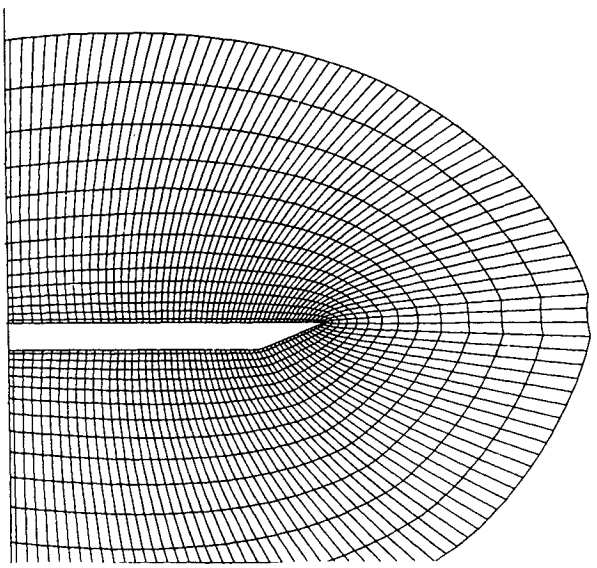

Fig. 2 Computational grid near the leading edge.

simpler domains on the basis of singular geometry points such as those defining the sharp-wing leading edge. A grid with a high degree of orthogonality is then generated for each of the simpler sections. The sections are matched smoothly at their common boundaries due to the nearly complete control of the grid in the vicinity of these boundaries. These capabilities result in highly orthogonal grid lines near sharp leading edges, as shown in Fig. 2.

To minimize possible solution sensitivity to grid density, the grid dimensions used were generally the largest attainable within the constraints of the McDonnell Douglas CRAY X-MP/18 computer. With these grids, a typical computational time for each Euler solution was on the order of one CPU hour. Figures 3 and 4 show typical SCRAMG grids for the 60-deg and 70-deg semispan delta wings. The upstream and downstream grid boundaries are located approximately 6 and

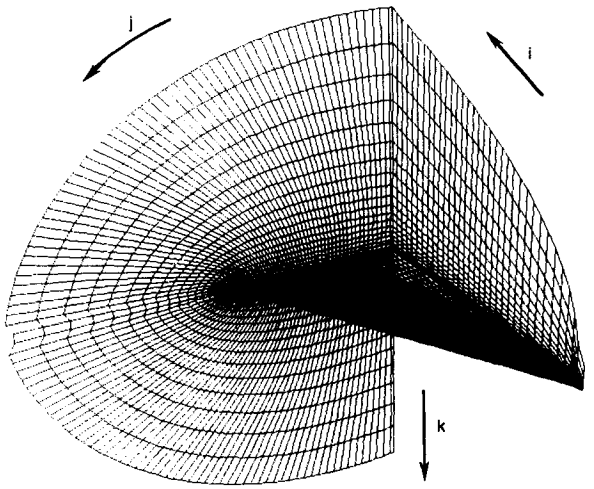

Fig. 3 Computational grid for 60-deg semispan delta wing ($i \times j \times k = 54 \times 113 \times 29$, half-plane).

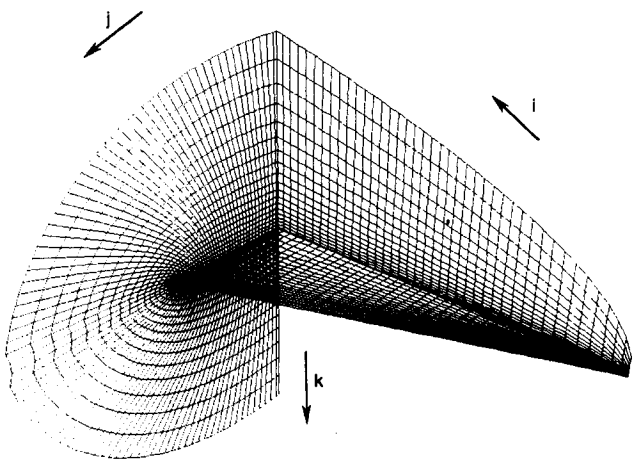

Fig. 4 Computational grid for 70-deg semispan delta wing ($i \times j \times k = 62 \times 89 \times 33$, half-plane).

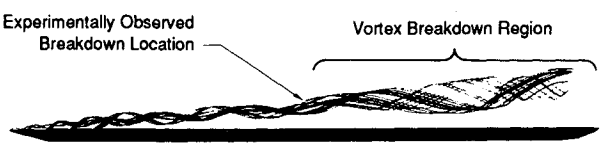

Fig. 5 Euler solution particle traces, 60-deg delta wing, angle of attack = 16 deg.

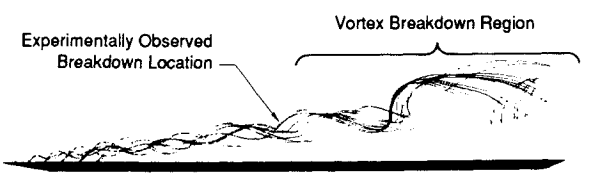

Fig. 6 Euler solution particle traces, 70-deg delta wing, angle of attack = 30 deg.

20 root chords, respectively, from the leading and trailing edges of the wing. The far-field boundary is located approximately 3 root chords from the surface of the wing. Approximately 67% of the axial planes intersect the wing surface with the remainder dispersed proportionately upstream of the wing and in the wake region. The 70-deg delta-wing grid shown in Fig. 4 contains 75% more nodes than the fine grid used in the delta-wing Euler computations of Raj, Sikora, and Keen, which showed some solution sensitivity to relatively coarse grid densities.[4]

Vortex Breakdown Onset

Before the vortex breakdown issues were studied, the ability of the CFL3D Euler code to predict the formation and subsequent roll-up of the leading-edge shear-layer was established. Figures 5 and 6 show Euler code particle traces that outline portions of the leading-edge vortices on 60-deg and 70-deg delta wings at angles of attack for which breakdown is observed over the wing in the experimental flow visualization data.[12] Because the computations made no attempt to model the boundary layer on the wing surface, no secondary vortex is observed in the Euler solutions.

In many cases, particularly at higher angles of attack, the well-defined leading-edge vortex degenerated rapidly into a substantially larger, more diffuse vortical flow region with relatively mild gradients. The presence of such an unsteady effect corresponded to less solution convergence, although it was almost always possible to achieve convergence of integrated delta-wing forces and moments. Figures 7 and 8 show convergence characteristics and lift histories for Euler solutions of the 60-deg and 70-deg delta-wing flowfields, respectively. In both cases, the vortex breakdown-like effect occurs near the 50% root-chord position.

The occurrences of such breakdown-like events in the Euler solutions were found to follow definite trends with angle of attack, and as such, were clearly not coincidental. To determine the relationship of this effect to the experimentally observed vortex breakdown phenomenon, it became necessary to move from subjective observation to a more quantitative basis for analysis.

In searching for clear and consistent criteria to identify the precise point of vortex breakdown, a straightforward and reliable technique was developed that identifies the onset of vortex breakdown in both CFD solutions and in experimental databases. This technique is based on the local flow swirl angle, which is defined as the arctangent of the circumferential velocity component divided by the axial velocity component. These velocity data are readily available from both the LDV

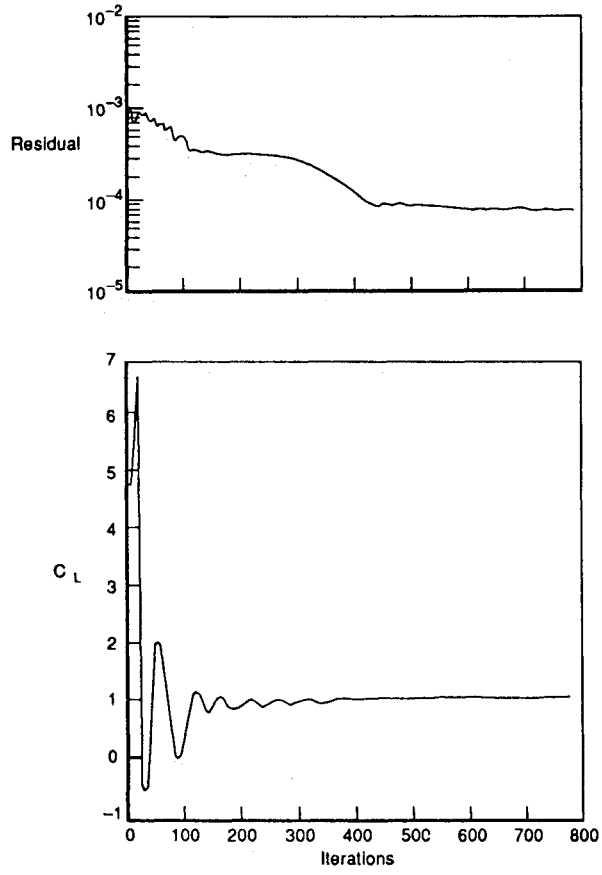

Fig. 8 Euler solution residual and lift histories, 70-deg delta wing, angle of attack = 30 deg.

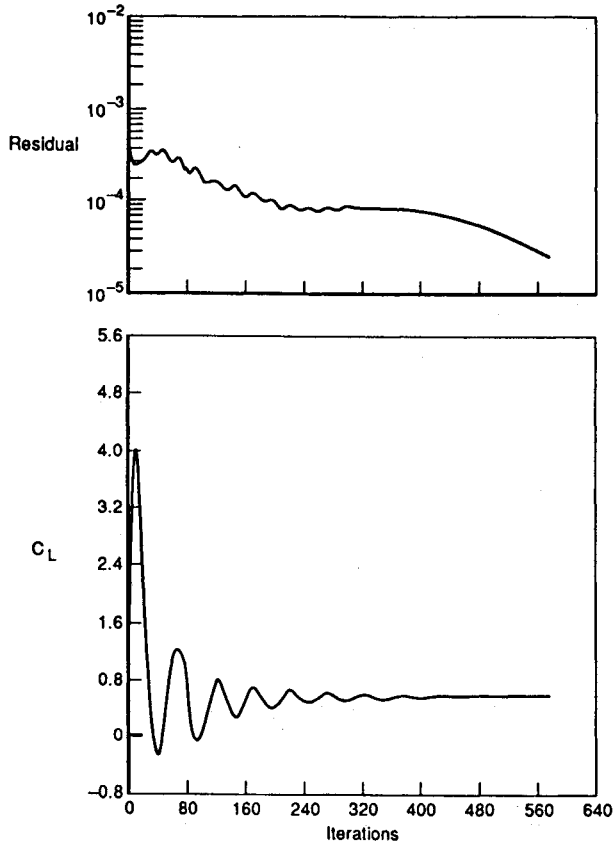

Fig. 7 Euler solution residual and lift histories, 60-deg delta wing, angle of attack = 16 deg.

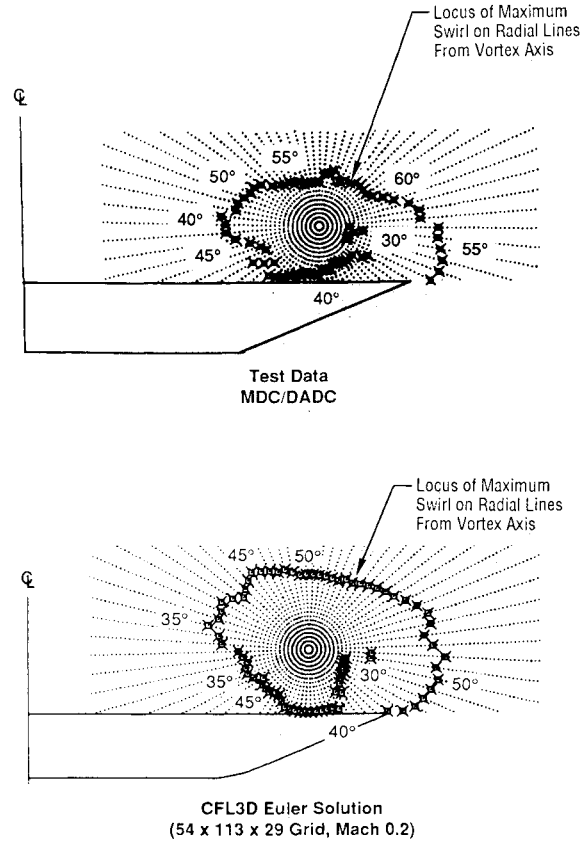

Fig. 9 Comparison of vortex shear-layer prediction with test data, 60-deg delta wing, angle of attack = 20 deg, $x/c_r = 0.20$.

database and the Euler solutions. According to conventional vortex theories, the maximum vortex swirl (or helical angle) is located at the edge of a symmetrical vortex core, and is constant along the core perimeter.[17,18] However, a complementary experimental effort has shown that for a vortex in the presence of a wing surface, the maximum swirl angle (in any given direction away from the vortex axis) is actually in the shear layer that emanates from the wing leading edge.[11] Not only is this effect observed in the test data, it is also predicted quite accurately by the Euler code. Figures 9 and 10 compare Euler predictions of the leading-edge shear layers for the 60-deg and 70-deg delta wings, respectively, with test data. The vortex core location was determined in each case by the position of the minimum total pressure. The values of the swirl angle at various points along the shear layer are also shown in Figs. 9 and 10 to provide a measure of Euler code accuracy in predicting local flow angularity.

At the onset of vortex breakdown, the locus of maximum swirl angle, which had outlined the shear layer prior to breakdown, falls in toward the vortex axis as shown in Fig. 11. This localized apparent "collapse" of the shear layer in the Euler solution precedes a rapid disintegration of the well-defined vortex structure into a diffuse, vortical wake-like flow structure resembling the experimentally observed breakdown phenomenon. The initial point of this collapse does not seem to be restricted to any one circumferential position, although the tendency was to favor the lower inboard quadrant of the vortex as represented in Fig. 11. Figure 12 shows a view of a collapsing locus of maximum swirl angle at vortex breakdown onset as obtained from the LDV data. The ability to observe such an effect in experiment is highly dependent on the positioning of the LDV measurement planes because the collapse is very rapid, occurring over a small fraction of the root chord.

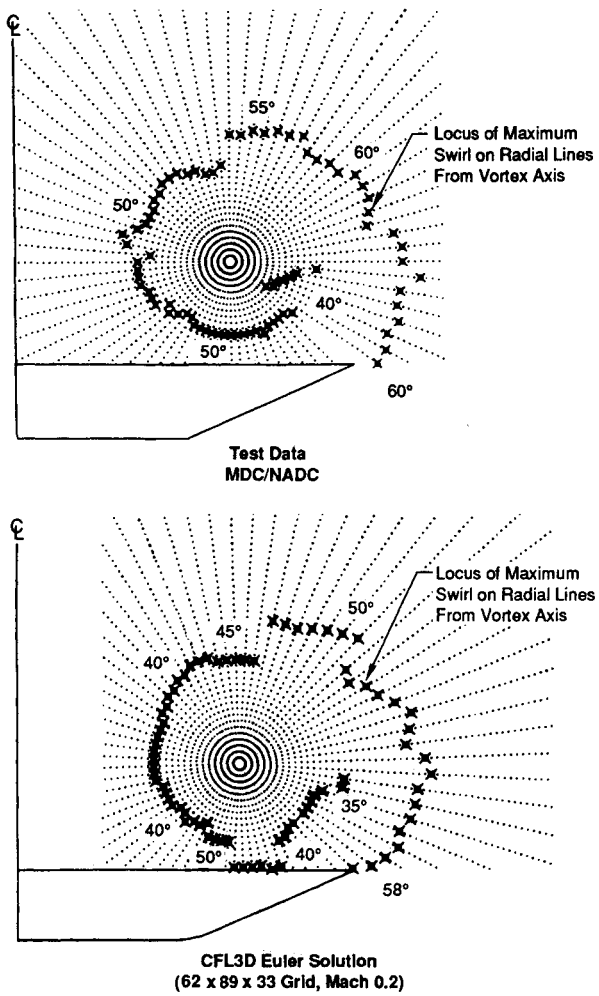

Fig. 10 Comparison of vortex shear-layer prediction with test data, 70-deg delta wing, angle of attack = 33 deg, $x/c_r = 0.20$.

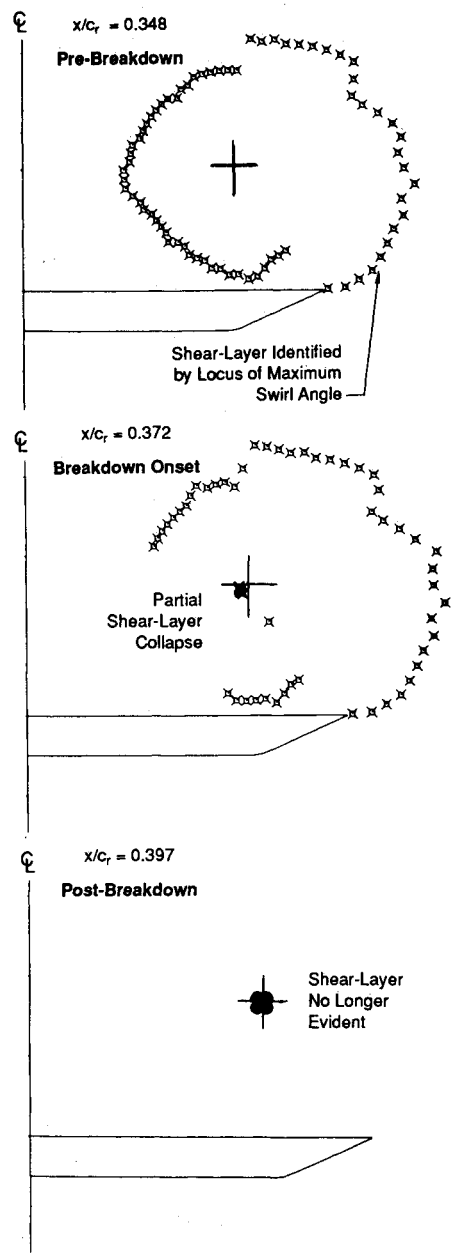

Fig. 11 Identifying vortex breakdown from locus of swirl angle in a Euler solution, 70-deg delta wing, angle of attack = 33 deg.

Because this apparent shear-layer collapse is evident in all the Euler solutions exhibiting breakdown studied, a straightforward and consistent method of identifying the onset of vortex-breakdown is thus defined. The degree of precision in the technique is limited by the amount of available data because the collapse will be observed between two adjacent data planes (i.e., constant root-chord grid planes in the Euler solutions). Because it is not possible to locate vortex breakdown precisely within a grid cell bordered by these grid planes, the cell midpoint is chosen to represent the breakdown location.

Breakdown Progression with Angle of Attack

Several Euler calculations were obtained for an angle of attack range where vortex breakdown is observed in experimental data. The point of predicted vortex breakdown (chordwise location of apparent shear-layer collapse) moves toward the delta-wing apex with increasing angle of attack, a trend consistent with test data. Initial investigations of vortex breakdown sensitivity to computational grid characteristics showed

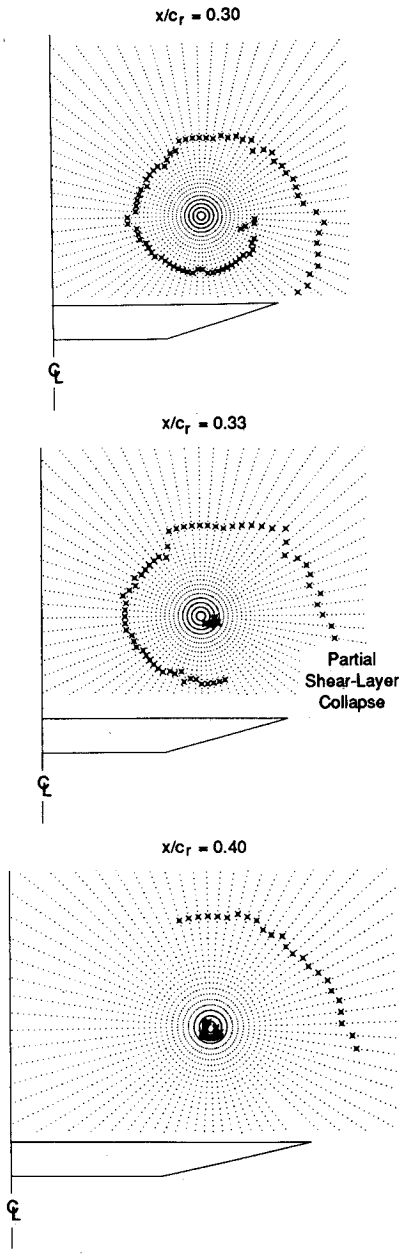

Fig. 12 Identifying vortex breakdown from locus of swirl angle, test data MDC/NADC, 70-deg delta wing, angle of attack = 33 deg.

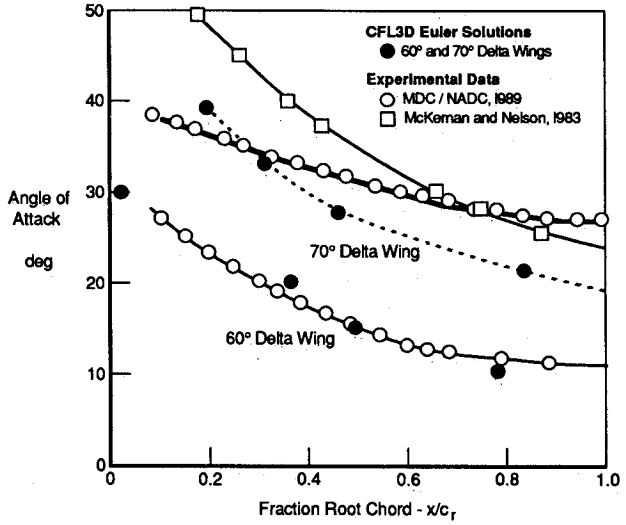

Fig. 13 Comparison of predicted vortex breakdown progression with test data.

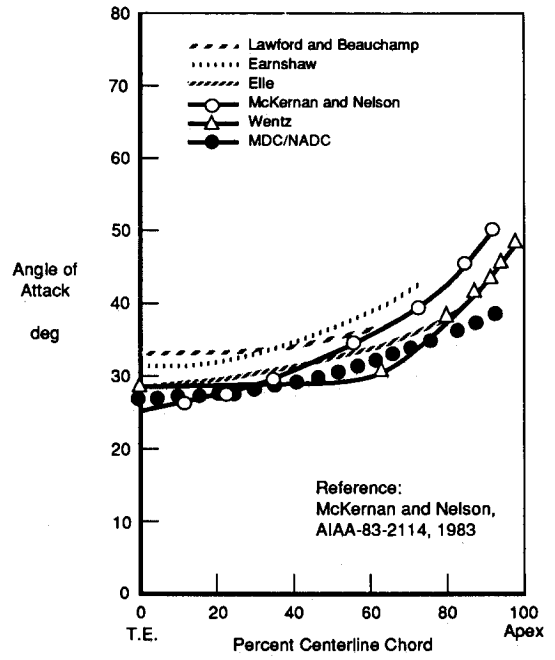

Fig. 14 Vortex breakdown progressions from various 70-deg delta-wing experiments.

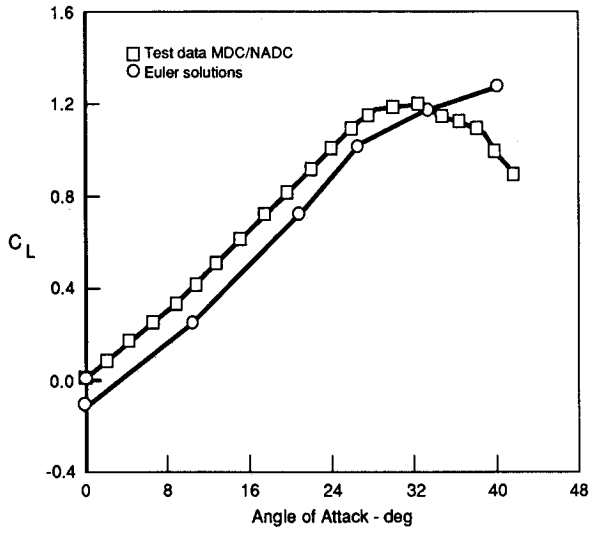

Fig. 15 Comparison of lift-curve prediction with test data, 70-deg delta wing.

only small effects. However, this finding must be considered inconclusive until a more thorough study into these effects is conducted. Figure 13 shows predicted vortex breakdown locations as a function of angle of attack for the 60-deg and 70-deg delta wings. Also shown are the breakdown progressions obtained in the MDC/NADC vortex flowfield investigation, which were determined through laser light-sheet flow visualization.[12] Some unsteadiness in the experimentally observed breakdown resulted in breakdown location uncertainty of approximately 3% root chord. The 60-deg delta-wing breakdown locations are shown to have better agreement with experiment than the 70-deg wing data.

The accuracy of the Euler predictions are more fully appreciated by considering the sensitive nature of vortex breakdown to the test environment. The vortex breakdown progression of McKernan and Nelson[19] is also shown in Fig. 13 to provide a better perspective for evaluating the accuracy of the Euler predictions. The 70-deg delta wing tested by McKernan and Nelson[19] is identical in planform to the MDC/NADC wing, but has a 65-deg lower-surface bevel and a squared trailing edge, making the wing considerably more

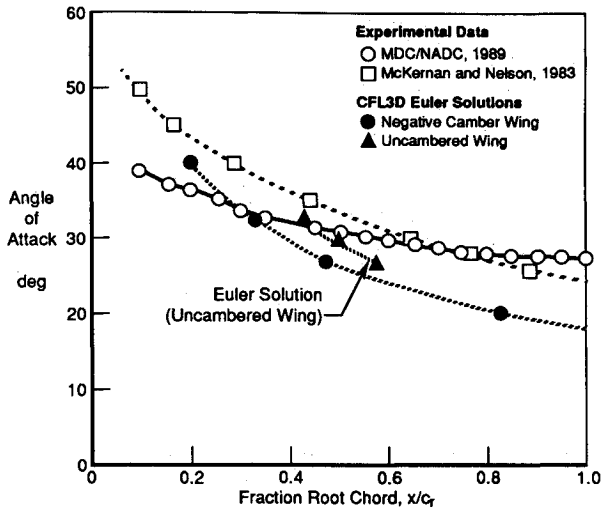

Fig. 16 Comparison of predicted vortex breakdown progression for cambered and uncambered 70-deg delta wing.

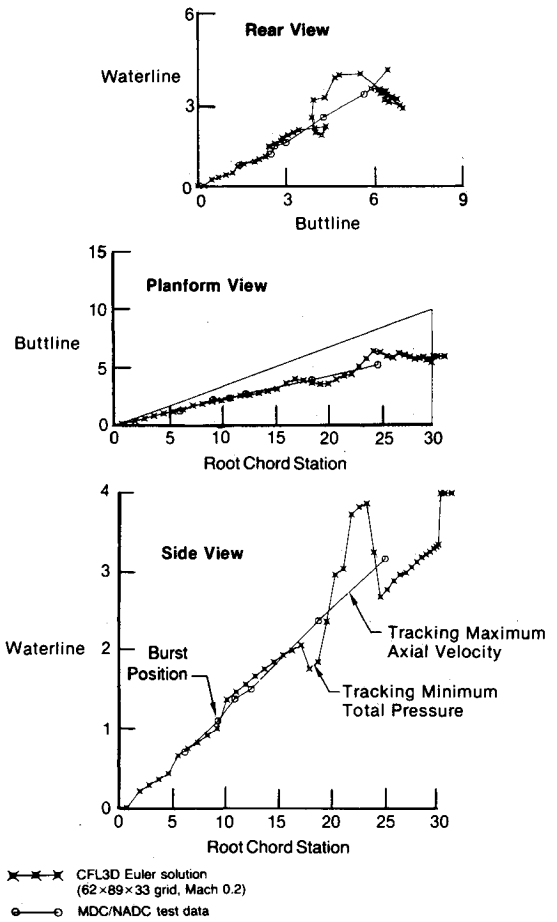

Fig. 17 Comparison of vortex trajectory prediction with test data, 70-deg delta wing, angle of attack = 33 deg.

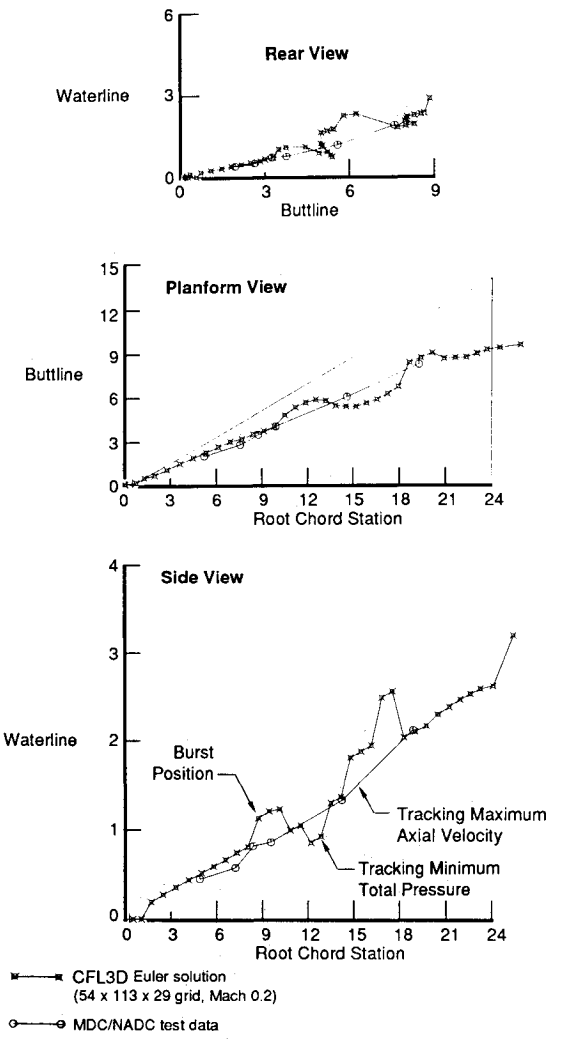

Fig. 18 Comparison of vortex trajectory prediction with test data, 60-deg delta wing, angle of attack = 20 deg.

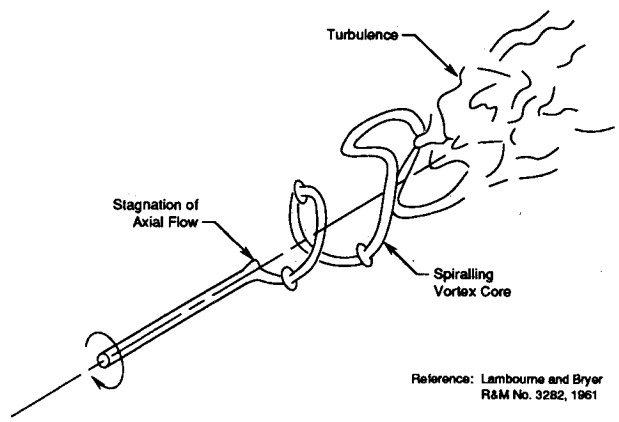

Fig. 19 Spiral-type vortex breakdown observed in experiments.

blunt by comparison. Figure 14 (modified from McKernan and Nelson) shows breakdown progressions for several experiments involving 70-deg delta wings. The principal reasons for the wide variation in breakdown location are as yet unclear, although leading- and trailing-edge geometry details, wing thickness, tunnel blockage effects, and model support effects are likely contributors.[19,20]

If details of the delta-wing geometry are important to experimentally observed vortex breakdown characteristics, then they should be equally important to any attempts to simulate the problem numerically. For example, Fig. 15 compares the lift-curve predicted by the Euler code through the entire range of angles of attack where vortex breakdown is present over the wing. The lift-curve slope agreement is good, although the Euler code predicts an angle-of-zero-lift of approximately 4 deg, which is not observed in the test data. This discrepancy sheds light on an inherent limitation of Euler codes. Because its inviscid formulation has no accounting for a viscous boundary layer, the Euler code does not predict the experimentally observed flow separation at the 25-deg trailing-edge bevel. As a result, the attached-flow Euler solutions of Fig. 13 reflect the significant negative camber created by the leading- and

trailing-edge bevels. This camber causes a positive shift in the lift-curve relative to the test data. The effect of this camber on predicted breakdown progression was evaluated by analyzing a 70-deg delta wing with symmetrical upper and lower surface bevels at both the leading and trailing edges. In Fig. 16 the predicted vortex breakdown progression is compared to data from the cambered baseline wing, showing a shift in breakdown location of approximately 10% root chord for the angles of attack investigated.

Trajectory of the Vortex Core

Figures 17 and 18 show Euler code predictions of vortex trajectory compared to experimental data for the 60-deg and 70-deg delta wings, respectively. In all cases studied, the vortex trajectories agreed very closely to experimental data and were determined to be relatively insensitive to computational grid density. Prior to breakdown, the vortex axis was identified in the Euler solution by locating the point of minimum total pressure. Total pressure losses accompany any solution of the discrete Euler equations and originate from numerical dissipation (e.g., truncation error), which is common to all Euler methods, and from explicit applications of artificial viscosity.

The spiraling trajectory exhibited in the solutions after breakdown (see Figs. 17 and 18) results from the minimum total pressure point being driven off the axis of the postbreakdown rotational flow. The sense of the spiral rotation is opposite to the sense of rotation of the primary vortex core. This effect closely resembles the spiraling of the vortex core after breakdown, sketched in Fig. 19, which is often observed in vortex breakdown experiments involving delta wings.[20-22]

Conclusions

The ability of numerical methods based on the Euler equations to model a vortex breakdown-like effect that closely follows experimental data trends is not coincidental. A method has been described that precisely identifies the point of breakdown onset, thus, allowing for quantitative comparison of breakdown predictions with experimental data. By keeping in mind the sensitive nature of breakdown location to details of the computational and experimental environments, the basic quality of Euler predictions indicates that leading-edge vortex breakdown is governed primarily by inviscid factors. It is not suggested that the unsteady, turbulent flow in the postbreakdown region is appropriately modeled with the Euler equations. However, the breakdown mechanism itself, seems to be within reach of the inviscid theory. Furthermore, the numerical dissipation inherent to the Euler code, seems to provide a qualitatively reasonable description of the postbreakdown flow.

Acknowledgments

The authors gratefully acknowledge the cooperation of Marvin Walters of the Naval Air Development Center regarding the use of the experimental vortex flowfield data presented herein. Gratitude is also extended to Frederick Roos and Jerome Kegelman of the McDonnell Douglas Research Laboratories for many valuable discussions. Finally, the authors thank David Halt, Robert Lowrie, and Robert O'Nell for their assistance in the grid generation efforts and in CFL3D code operation.

References

[1]McMillin, S. N., Thomas, J. L., and Murman, E. M., "Euler and Navier-Stokes Solutions for the Leeside Flow Over Delta Wings at Supersonic Speeds," AIAA Paper 87-2270, Aug. 1987.

[2]Rizzi, A., Bernhard, M., and Purcell, C. J., "Comparison of Euler and Navier-Stokes Solutions for Vortex Flow Over a Delta Wing," AIAA Paper 87-2347, Aug. 1987.

[3]Raj, P., and Long, L. N., "An Euler Aerodynamic Method for Leading-Edge Vortex Flow Simulation," Vortex Flow Aerodynamics Conference, NASA-Langley Research Center, Oct. 8–10 1985.

[4]Raj, P., Sikora, J. S., and Keen, J. M., "Free-Vortex Flow Simulation Using a Three-Dimensional Euler Aerodynamic Method," *Journal of Aircraft*, Vol. 25, No. 2, 1988, pp. 128–134.

[5]Hitzel, S. M., and Schmidt, W., "Slender Wings with Leading-Edge Vortex Separation: A Challenge for Panel Methods and Euler Solvers," *Journal of Aircraft*, Vol. 21, No. 10, 1984, pp. 751–759.

[6]Rizzi, A., and Purcell, C. J., "Numerical Experiment with Inviscid Vortex-Stretched Flow Around a Cranked Delta Wing: Subsonic Speed," AIAA Paper 85-4080, Oct. 1985.

[7]Hitzel, S. M., "Wing Vortex-Flows Up Into Vortex-Breakdown, A Numerical Simulation," AIAA Paper 88-2518-CP, June 1988.

[8]Brandt, S. A., "Numerical Simulation of Leading-Edge Vortex Rollup and Bursting," Ph.D. Dissertation, Univ. of Illinois at Urbana-Champaign, Urbana, IL, 1988.

[9]Bossel, H. H., "Stagnation Criterion for Vortex Flows," AIAA Journal, Vol. 6, No. 6, 1968, pp. 1192–1193.

[10]Bryce, S. G., "A New Analytical Approach to Vortex Breakdown Investigation," AIAA Paper 87-2495, Aug. 1987.

[11]O'Neil, P. J., et al., "Investigation of Flow Characteristics of a Developed Vortex," NADC Report No. NADC-89114-60, May 1989.

[12]Roos, F. W., and Kegelman, J. T., "An Experimental Investigation of Sweep-Angle Influence on Delta-Wing Flows," AIAA Paper 90-0383, Jan. 1990.

[13]Kegelman, J. T., and Roos, F. W., "The Flowfields of Bursting Vortices Over Moderately Swept Delta Wings," AIAA Paper 90-0599, Jan. 1990.

[14]Thomas, J. L., Taylor, S. L., and Anderson, W. K., "Navier-Stokes Computations of Vortical Flows Over Low Aspect Ratio Wings," AIAA Paper 87-0207, Jan. 1987.

[15]Verhoff, A., and O'Neil, P. J., "Accurate, Efficient Prediction Method for Supersonic/Hypersonic Inviscid Flow," AIAA Paper 87-1165, June 1987.

[16]Thompson, J. F., Thames, F. C., and Mastin, C. W., "Automatic Numerical Generation of Body-Fitted Curvilinear Coordinate System for Field Containing Any Number of Arbitrary Two-Dimensional Bodies," *Journal of Computational Physics*, Vol. 15, No. 3, 1974, pp. 299–319.

[17]Bossel, H. H., "Vortex Breakdown Flowfield," *Physics of Fluids*, Vol. 12, No. 3, 1969, pp. 498–508.

[18]Luckring, J. M., "A Theory for the Core of a Three-Dimensional Leading-Edge Vortex," AIAA Paper 85-0108, Jan. 1985.

[19]McKernan, J. F., and Nelson, R. C., "An Investigation of the Breakdown of the Leading Edge Vortices on a Delta-Wing at High Angles of Attack," AIAA Paper 83-2114, Aug. 1983.

[20]Kegelman, J. T., and Roos, F. W., "Effects of Leading-Edge Shape and Vortex Burst on the Flowfield of a 70-Degree-Sweep Delta Wing," AIAA Paper 89-0086, Jan. 1989.

[21]Payne, F. M., Ng, T. T., and Nelson, R. C., "Visualization and Flow Surveys of the Leading Edge Vortex Structure on Delta Wing Planforms," AIAA Paper 86-0330, Jan. 1986.

[22]Lambourne, N. C., and Bryer, D. W., "The Bursting of Leading-Edge Vortices—Some Observations and Discussion of the Phenomenon," Aeronautical Research Council R&M 3282, April 1961.